BIOLOGICAL CRYSTALLOGRAPHY
ISSN 1399-0047

Two crystal structures of the FK506-binding domain of *Plasmodium falciparum* FKBP35 in complex with rapamycin at high resolution

Alessandra Bianchin,[a] Frederic Allemand,[b] Angus Bell,[c] Anthony J. Chubb[a] and Jean-François Guichou[b]*

[a]Conway Institute of Biomolecular and Biomedical Science, University College Dublin, Dublin, Ireland, [b]Centre de Biochimie Structurale, CNRS UMR5048, INSERM U1054, Université de Montpellier, Montpellier, France, and [c]Department of Microbiology, School of Genetics and Microbiology, Moyne Institute, Trinity College Dublin, Dublin, Ireland. *Correspondence e-mail: guichou@cbs.cnrs.fr

Received 18 November 2014
Accepted 26 March 2015

Edited by P. Langan, Oak Ridge National Laboratory, USA

Keywords: *Plasmodium falciparum*; FK506-binding domain; *Pf*FKBP35; rapamycin; antimalarial drug.

PDB references: FK506-binding domain of FKBP35, complex with rapamycin, 4qt2; 4qt3

Supporting information: this article has supporting information at journals.iucr.org/d

Antimalarial chemotherapy continues to be challenging in view of the emergence of drug resistance, especially artemisinin resistance in Southeast Asia. It is critical that novel antimalarial drugs are identified that inhibit new targets with unexplored mechanisms of action. It has been demonstrated that the immunosuppressive drug rapamycin, which is currently in clinical use to prevent organ-transplant rejection, has antimalarial effects. The *Plasmodium falciparum* target protein is *Pf*FKBP35, a unique immunophilin FK506-binding protein (FKBP). This protein family binds rapamycin, FK506 and other immunosuppressive and non-immunosuppressive macrolactones. Here, two crystallographic structures of rapamycin in complex with the FK506-binding domain of *Pf*FKBP35 at high resolution, in both its oxidized and reduced forms, are reported. In comparison with the human FKBP12–rapamycin complex reported previously, the structures reveal differences in the $\beta4$–$\beta6$ segment that lines the rapamycin binding site. Structural differences between the *Plasmodium* protein and human hFKBP12 include the replacement of Cys106 and Ser109 by His87 and Ile90, respectively. The proximity of Cys106 to the bound rapamycin molecule (4–5 Å) suggests possible routes for the rational design of analogues of rapamycin with specific antiparasitic activity. Comparison of the structures with the *Pf*FKBD–FK506 complex shows that both drugs interact with the same binding-site residues. These two new structures highlight the structural differences and the specific interactions that must be kept in consideration for the rational design of rapamycin analogues with antimalarial activity that specifically bind to *Pf*FKBP35 without immunosuppressive effects.

1. Introduction

Malaria is still one of the most significant human diseases worldwide, with estimates of 124–283 million cases and 367 000–755 000 deaths in 2014, mostly in sub-Saharan Africa (World Health Organization, 2015; White *et al.*, 2014). The disease is caused by infection with intracellular parasites of the apicomplexan protozoon *Plasmodium*. *P. falciparum* is the most lethal pathogen among the five species that affect humans and it has developed resistance to several antimalarial drugs (White, 2004). The identification of new chemotherapeutic targets and lead compounds will be an important element of the ongoing campaign to eradicate malaria. It has previously been shown that the macrolactone immunosuppressants FK506 and rapamycin (Figs. 1*a* and 1*b*) and several non-immunosuppressive FK506 congeners have antimalarial activity (Bell *et al.*, 1994; Monaghan *et al.*, 2005). The apparent receptor in *P. falciparum* is a 35 kDa FK506-binding protein, *Pf*FKBP35 (Braun *et al.*, 2003; Monaghan & Bell,

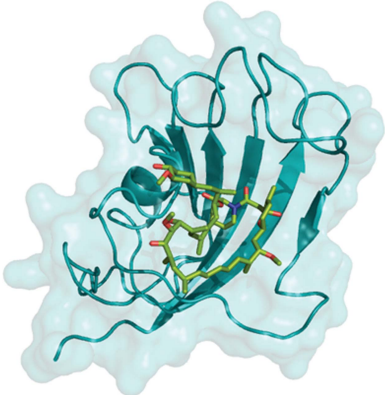

2005; Kumar *et al.*, 2005). The natural functions of FKBPs have seldom been elucidated, but most family members, including *Pf*FKBP35, possess peptidyl–prolyl *cis–trans* isomerase (PPIase) activity (Galat, 2003; Monaghan & Bell, 2005; Kumar *et al.*, 2005) and some can act as molecular chaperones (Kuzuhara & Horikoshi, 2004; Monaghan & Bell, 2005), both of which are relevant to protein folding. Among the physiological roles demonstrated for FKBPs are receptor signalling (Riggs *et al.*, 2003), calcium homeostasis (Jayaraman *et al.*, 1992; Cameron *et al.*, 1995), transcription (Yang *et al.*, 1995), protein trafficking and stability (Shirane & Nakayama, 2003; Jinwal *et al.*, 2010; Ahearn *et al.*, 2011), and neuroprotection (Edlich *et al.*, 2006). FKBP ligands are being explored as potential therapies for various diseases. For example, rapamycin and its derivatives are under investigation for the treatment of cancer, tuberculosis, Alzheimer's disease, lupus erythematosus and muscular dystrophy (Blackburn & Walkinshaw, 2011).

Unlike most eukaryotes characterized to date, *Plasmodium* lacks a simple single FK506-binding domain (FKBD) protein like the major human FKBP hFKBP12. The FKBD of *Pf*FKBP35 shows 44% amino-acid sequence identity to hFKBP12 but has an additional tetratricopeptide repeat (TPR) domain and putative calmodulin-binding motif, making it reminiscent of, if not clearly homologous to, certain other human FKBPs, namely FKBP38, FKBP51 and FKBP52. Human FKBP12 is the major receptor for both FK506 and rapamycin, but the mechanisms of action of the two drugs are markedly different. The hFKBP12–FK506 complex allows the formation of a ternary complex with the phosphoprotein serine/threonine phosphatase calcineurin (CaN; PPP3), inhibiting the phosphatase activity and blocking T-cell activation. By contrast, the complex of FKBP12 and rapamycin interacts with the protein serine/threonine kinase mammalian target of rapamycin (mTOR). This complex inhibits the biochemical pathways required for cell-cycle progression during T-cell proliferation and blocks cytokine signal transduction. *Pf*FKBP35, despite its similarity in domain architecture to the noncanonical FKBP38, could be considered to have a canonical FKBD because it interacts with both FK506 and rapamycin and possesses the conserved residues in the active site (Fig. 1*c*). The PPIase activity of *Pf*FKBP35 is inhibited by FK506 and rapamycin, with IC_{50} values of 0.32 and 0.48 μM, respectively (Monaghan & Bell, 2005).

Unusually, calcineurin phosphatase activity is inhibited by *Pf*FKBP35 in the absence of FK506, at least under some experimental conditions (Monaghan & Bell, 2005; Kumar *et al.*, 2005), suggesting that the antimalarial activity of FK506 may not be mediated by *Plasmodium* CaN. In the case of rapamycin, any analogy between the immunosuppressive and antimalarial actions appears to be ruled out by the absence of mTOR in *Plasmodium*. This cumulative evidence points to *Pf*FKBP35 as a possible new antimalarial target acting through an unexplored mechanism of action. Previously, Kotaka and coworkers characterized the X-ray structure of the complex of FK506 bound to the FKBD of *Pf*FKBP35

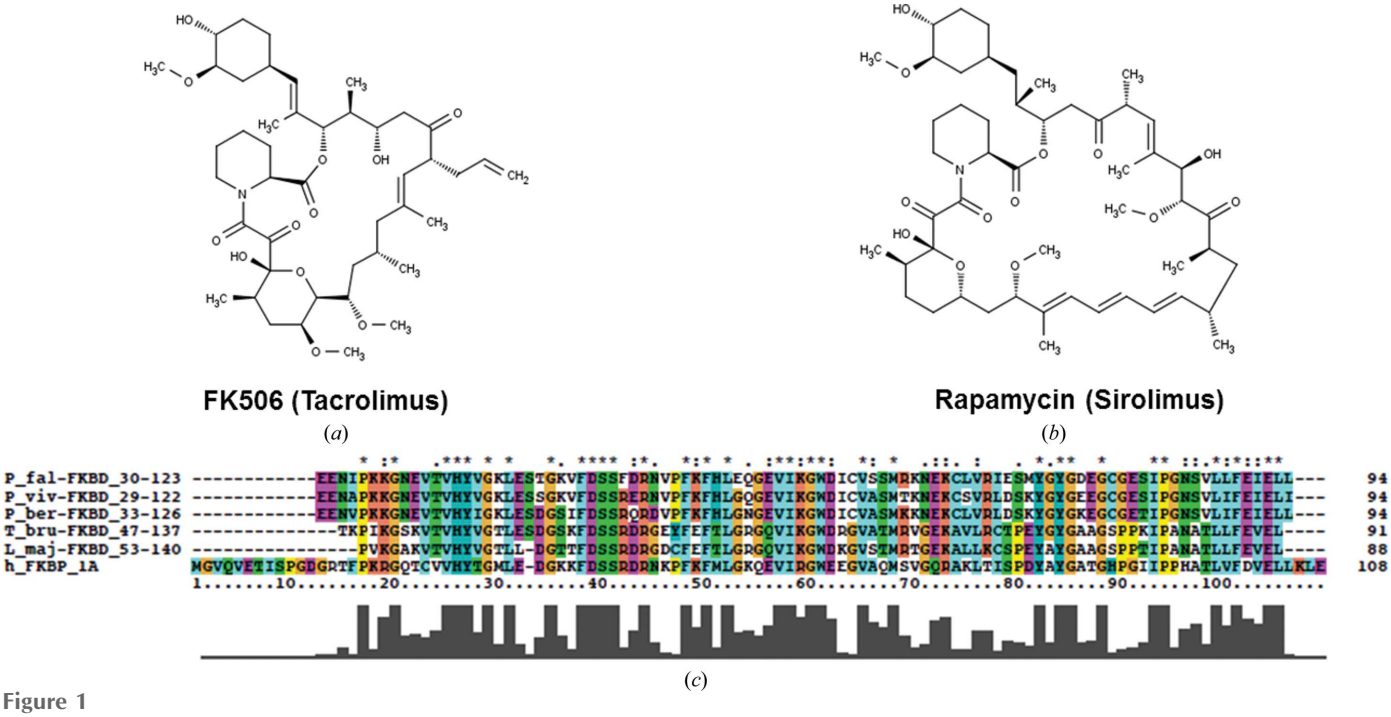

Figure 1
Chemical structures of immunosuppressant drugs and alignment of selected FKBP proteins. (*a*) Chemical structure of FK506. (*b*) Chemical structure of rapamycin. (*c*) Alignment of the *P. falciparum* FK506-binding domain with other FKBDs present in different protozoan parasites and with human FKBP12 (made with *ClustalX*; Larkin *et al.*, 2007). P_fal-FKBD_30–123: *P. falciparum* (strain 3D7), NCBI entry XP_001350859.1, FKB domain, amino acids 30–123. P_viv-FKBD_29–122: *P. vivax* (strain Sal1), NCBI entry XP_001613999.1, FKB domain, amino acids 29–122. P_ber-FKBD_33–126: *P. berghei* (strain ANKA), NCBI entry XP_672280.1, FKB domain, amino acids 33–126. T_bru-FKBD_47–137: *Trypanosoma brucei* (strain TREU927), NCBI entry XP_828079.1, FKB domain, amino acids 47–137. L_maj-FKBD_53–140: *Leishmania major* (strain Friedlin), NCBI entry XP_001682742.1, FKB domain, amino acids 53–140. h_FKBP_1A: human FKB1A protein, UniProt code P62942, full length.

(Kotaka *et al.*, 2008), and this structure was used as a basis for the design of new antimalarial FKBP ligands (Harikishore, Leow *et al.*, 2013; Harikishore, Niang *et al.*, 2013). In this work, we have elucidated the X-ray structure of rapamycin bound to the FKBD of *Pf*FKBP35 in two orthorhombic crystal forms for the oxidized and reduced forms of FKBD to high resolutions of 1.44 and 1.40 Å, respectively, which might provide valuable clues for the design of novel non-immunosuppressive agents specific for the *Plasmodium* protein. Drugs based on this model should thus retain the antimalarial activities of FK506 and rapamycin, while avoiding their immunosuppressive effects. We compare these structures with the previously reported structure of the human FKBP12–rapamycin complex. In spite of a similar ligand-binding site to that of hFKBP12, the *Pf*FKBD structures reveal subtle differences in the $\beta4$–$\beta6$ region that lines the rapamycin binding pocket. Of note, two of its residues are 4–5 Å from the nearest atom of the ligand, providing opportunities to alter the rapamycin compound to increase its specificity for *Pf*FKBP35.

2. Materials and methods

2.1. Protein expression and purification

Protein expression was performed with the pET29-*Pf*FKBD plasmid (Yoon *et al.*, 2007), a kind gift from Professor H. S. Yoon, Nanyang Technological University, Singapore. This vector was transformed into *Escherichia coli* BL21(DE3) cells and the transformed cells were grown overnight at 25°C in ZYM-5052 auto-induction medium (Studier, 2005) supplemented with kanamycin (50 µg ml^{-1}). Cells were harvested by 15 min centrifugation at 6000*g* at 4°C. The pellet was resuspended in 25 m*M* sodium phosphate buffer pH 7.5, 500 m*M* NaCl, 2 m*M* β-mercaptoethanol (buffer *A*) and stored at −80°C. Cells were lysed by sonication, and insoluble proteins and cell debris were sedimented by centrifugation at 40 000*g* at 4°C for 30 min. The supernatant was filtered through 0.45 µm filters and loaded onto affinity columns (HisTrap FF 5 ml, GE Life Sciences) equilibrated with buffer *A*. The columns were washed with 20 column volumes of buffer *A*. The protein was eluted with 20 column volumes of a linear 0–100% gradient of buffer *B* (buffer *A* containing 0.5 *M* imidazole) at 2 ml min^{-1}. The peak fractions were analysed by SDS–PAGE. Fractions containing *Pf*FKBD were pooled and dialysed overnight at 4°C against 20 m*M* Tris–HCl pH 8.0, 25 m*M* NaCl, 1 m*M* dithiothreitol (DTT) (buffer *C*). The dialysed protein was then loaded onto an anion-exchange column (HiTrap Q HP 5 ml, GE Life Sciences). *Pf*FKBD was eluted with 20 column volumes of a linear gradient (0–100%) from buffer *C* to buffer *D* (buffer *C* containing 1 *M* NaCl) at 2 ml min^{-1}. Fractions containing *Pf*FKBD were analysed by SDS–PAGE and pooled. The purified protein was dialysed against a conservation buffer consisting of 20 m*M* sodium phosphate buffer pH 6.8, 150 m*M* NaCl, 1 m*M* DTT, 1 m*M* tris(2-carboxyethyl)phosphine (TCEP), 0.01%(*w*/*v*) NaN_3 and was concentrated to 28 mg ml^{-1} with a Vivaspin centrifugal concentrator (Sartorius Stedim Biotech).

Table 1
Data-collection and refinement statistics for the *Pf*FKBD–rapamycin complex.

Values in parentheses are for the highest resolution shell.

PDB code	4qt2	4qt3
Data collection		
Space group	$P2_12_12_1$	$P2_12_12_1$
Unit-cell parameters (Å)	a = 35.8, b = 48.7, c = 58.9	a = 49.5, b = 50.2, c = 57.8
Wavelength (Å)	0.8726	0.97625
Resolution (Å)	30.60–1.44 (1.50–1.44)	50.15–1.40 (1.46–1.40)
Total reflections	75543	124923
Unique reflections	18930	28809
R_{merge}	0.072 (0.392)	0.032 (0.436)
$\langle I/\sigma(I)\rangle$	6.6 (2.0)	12.0 (1.8)
Completeness (%)	97.8 (89.2)	99.5 (99.4)
Multiplicity	3.9 (3.5)	3.7 (3.6)
Wilson B (Å^2)	12.5	17.9
Refinement		
Resolution (Å)	1.44	1.40
No. of reflections	17990	27343
R_{work}/R_{free} (%)	16.20/21.78	14.75/18.71
No. of atoms		
Protein	1002	1061
Rapamycin	65	65
Imidazole	5	—
Water	99	152
B factors (Å^2)		
Protein	16.27	21.79
Rapamycin	14.94	16.73
Imidazole	29.38	—
Water	29.65	34.49
Average B factor (Å^2)	17.38	23.05
R.m.s. deviations		
Bond lengths (Å)	0.012	0.006
Bond angles (°)	1.813	1.342
Ramachandran plot		
Most favoured regions (%)	98.3	98.3
Allowed regions (%)	1.7	1.7

2.2. Crystallization

Crystallization trials for the *Pf*FKBD–rapamycin complex were conducted with kits from Hampton Research and Qiagen using sitting-drop vapour diffusion at 18°C. Each trial utilized a Microlab STAR (Hamilton) and a Cartesian (Genomics Solutions) nano-dispensing robot with 200 nl drops (1:1 protein:well solution volume ratio) in 96-well sitting-drop plates. Several hits were found and crystals were obtained by mixing equal volumes of a well solution consisting of 0.1 *M* MIB buffer (sodium malonate, imidazole and boric acid in a 2:3:3 molar ratio) pH 7.0, 25%(*w*/*v*) PEG 1500 or 0.1 *M* MMT buffer (DL-malic acid, MES monohydrate and Tris base in a 1:2:2 molar ratio) pH 7.0, 25%(*w*/*v*) PEG 1500 with the *Pf*FKBP35–rapamycin solution (1:2 molar ratio). Crystals appeared 12–24 h later at 18°C, reaching 0.1 × 0.05 × 0.05 mm in size. Crystals were cryoprotected by gently removing most of the mother liquor followed by flash-cooling in liquid nitrogen.

2.3. Data collection, structure determination and refinement

Diffraction data were collected on the ID23-2 and ID-29 beamlines at the European Synchrotron Radiation Facility (ESRF) at 100 K and wavelengths of 0.8726 and 0.97625 Å to

resolutions of 1.44 and 1.40 Å, respectively. Data were processed using *XDS* (Kabsch, 2010) and scaled with *SCALA* (Winn *et al.*, 2011). The space group was determined to be $P2_12_12_1$ using *POINTLESS* (Evans, 2011) for both structures. With one subunit in the asymmetric unit for both structures, the Matthews coefficient (V_M) was calculated to be 2.12 Å^3 Da^{-1} with an estimated solvent content of 42% for the first structure and to be 2.45 Å^3 Da^{-1} with an estimated solvent content of 50% for the second structure (Kantardjieff & Rupp, 2003). The structures of the *Pf*FKBD–rapamycin complex were solved by molecular replacement with *MOLREP* (Vagin & Teplyakov, 2010) using the *Pf*FKBD–FK506 complex (PDB entry 2vn1; Kotaka *et al.*, 2008) as a search model (ligand and water molecules were removed). The structures were refined using *REFMAC*5 (Murshudov *et al.*, 2011) and model building was performed in *Coot* (Debreczeni & Emsley, 2012). All figures showing structures were produced using *PyMOL* (http://www.pymol.org/).

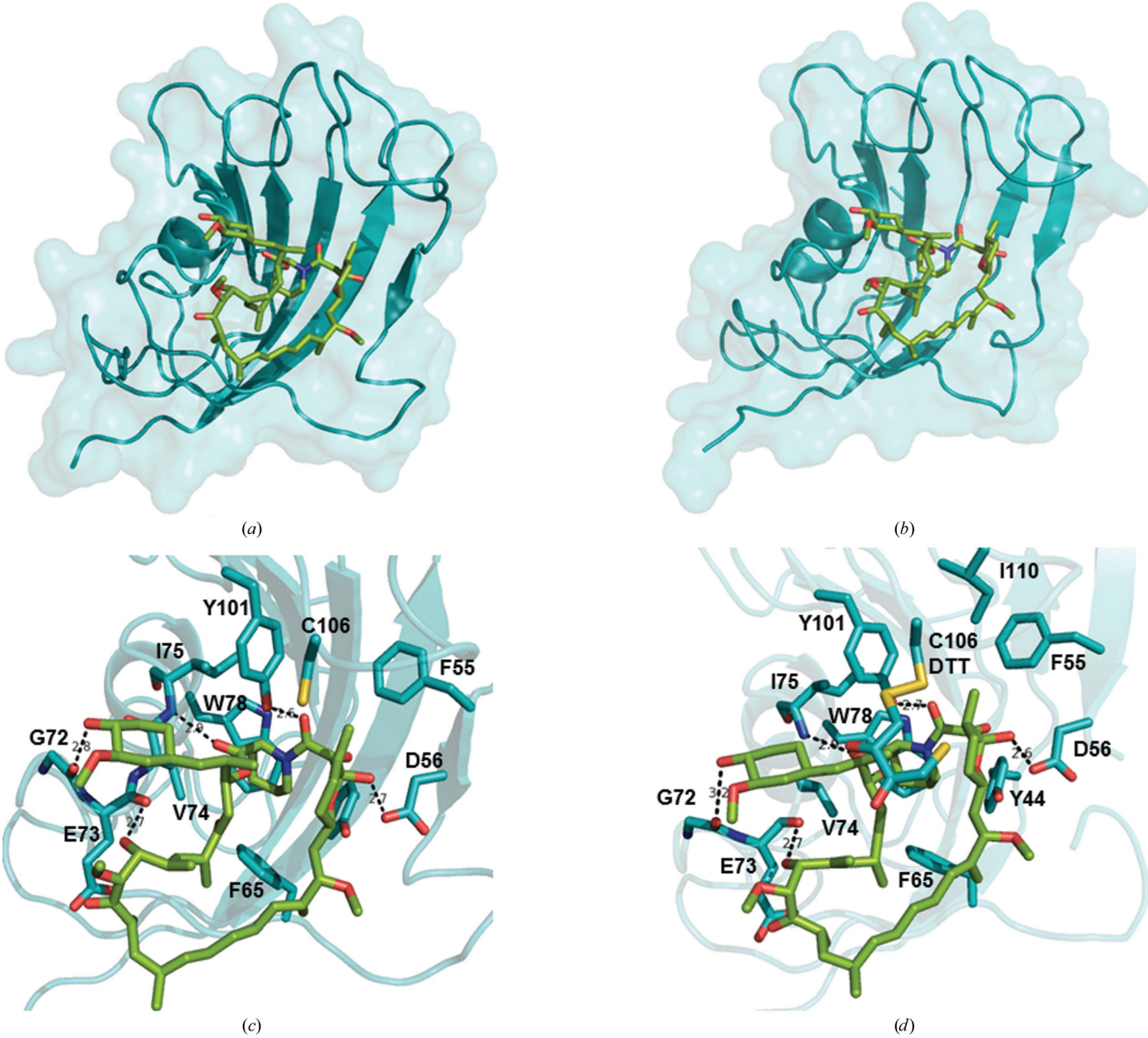

Figure 2
Structure of the *Pf*FKBD–rapamycin complex. (*a*) Cartoon and surface representations of the *Pf*FKBD and stick view of rapamycin (PDB entry 4qt2). (*b*) Cartoon and surface representations of the *Pf*FKBD and stick view of rapamycin (PDB entry 4qt3). (*c*) Enlargement of the binding pocket of rapamycin in *Pf*FKBD showing the binding residues as sticks and the hydrogen bonds as lines (PDB entry 4qt2). (*d*) Enlargement of the binding pocket of rapamycin in *Pf*FKBD showing the binding residues as sticks and the hydrogen bonds as lines (PDB entry 4qt3). (*e*) Schematic representation of the hydrogen-bond network of rapamycin and *Pf*FKBD (PDB entries 4qt2 and 4qt3). (*f*) View of the σ_A-weighted $2F_{obs} - F_{calc}$ electron-density OMIT map of rapamycin contoured at the 1.0σ level (blue; PDB entry 4qt2). (*g*) View of the σ_A-weighted $2F_{obs} - F_{calc}$ electron-density OMIT map of rapamycin contoured at the 1.0σ level (blue; PDB entry 4qt3).

Atomic coordinates and structures have been deposited in the Protein Data Bank with accession codes 4qt2 and 4qt3. Crystallographic data are summarized in Table 1.

3. Results

3.1. *Pf* FKBD–rapamycin complex preparation, crystallization and structure solution

We expressed *Pf*FKBD with a C-terminal His_6 tag for easy purification. Expression and subsequent purification produced highly pure protein with a typical yield of about 140 mg per litre of culture. The specific activity of the recombinant enzyme was measured by monitoring the *cis–trans* isomerization of the ALPF peptide (PPIase activity; Kofron *et al.*, 1991). We observed some crystallization hits (∼15) using the PACT kit from Qiagen. Two conditions [0.1 *M* MIB pH 7.0, 25%(*w*/*v*) PEG 1500 and 0.1 *M* MMT pH 7.0, 25%(*w*/*v*) PEG 1500] gave crystals with approximate dimensions of 100 × 50 × 50 µm. Two sets of data were obtained from these two crystals at 1.44 and 1.40 Å resolution and led to the structures deposited in the PDB as entries 4qt2 and 4qt3, respectively. These crystals belonged to the primitive orthorhombic space group $P2_12_12_1$, with unit-cell parameters a = 35.8, b = 48.7, c = 58.9 Å and a = 49.5, b = 50.2, c = 57.8 Å for PDB entries 4qt2 and 4qt3, respectively. Data-collection statistics are summarized in Table 1. The structures were solved by molecular replacement and one copy of *Pf*FKBD was found in the asymmetric unit for both structures. The final models consisted of 122 amino acids (residues 7–128) and 125 amino acids (residues 5–129), respectively.

3.2. Characteristics and comparison of the two *Pf* FKBD binding site–rapamycin complex structures

The *Pf*FKBD binding site is composed of an amphipathic six-stranded β-sheet (Figs. 2*a* and 2*b*) which has a right-handed twist and wraps around the helix, forming the

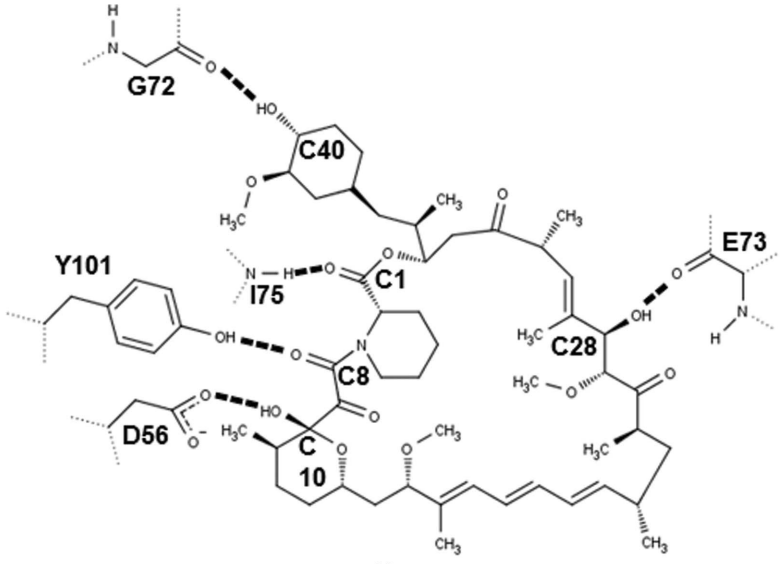

(*e*)

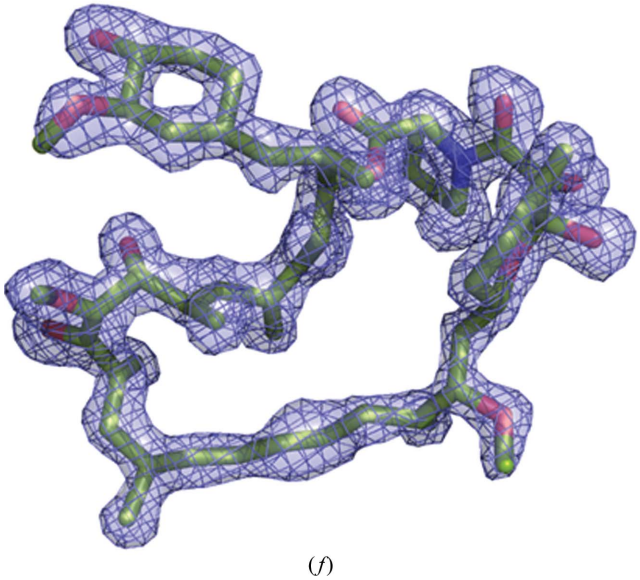

(*f*)

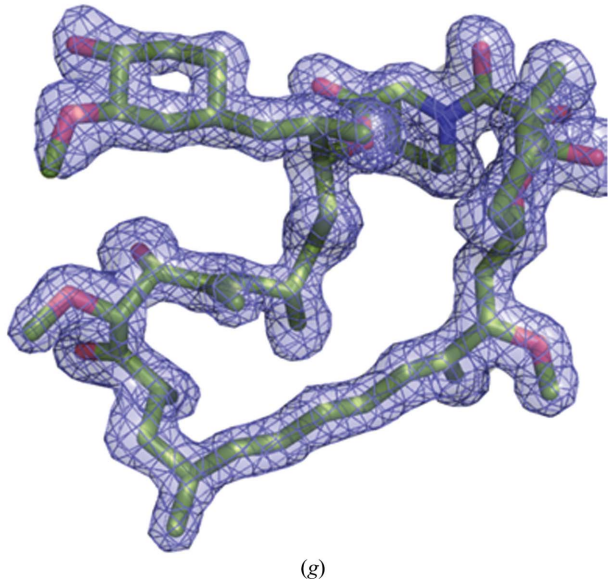

(*g*)

Figure 2 (continued)

hydrophobic pocket (Kang *et al.*, 2008; Kotaka *et al.*, 2008). We show here that the hydrophobic pocket between the α-helix and the β-sheet is the binding region for rapamycin, as is the case for FK506. The refined crystallographic structures contain 122 and 125 amino acids, respectively; owing to high mobility in the crystals some amino acids are missing from the N-terminal ends of each structure. Both structures present a monomeric structure of the *Pf*FKBD binding site in complex with rapamycin and clear density was observed for rapamycin (Figs. 2*f* and 2*g*). The two *Pf*FKBD–rapamycin structures are almost identical and can be superimposed with an r.m.s.d. of 0.23 Å on their C^{α} positions (Fig. 3*a*). The ligands present an r.m.s.d. of 0.18 Å (Fig. 3*b*). The ligand surface area is 2252 and 2253 $Å^2$, respectively, in the two structures. In both structures rapamycin forms hydrogen bonds to Asp56, Ile75, Gly72, Glu73 and Tyr101 (Figs. 2*c*, 2*d* and 2*e* and Table 2), which are generally conserved amino acids. Van der Waals interactions with a distance of less than 4.5 Å are listed in Table 2. Two

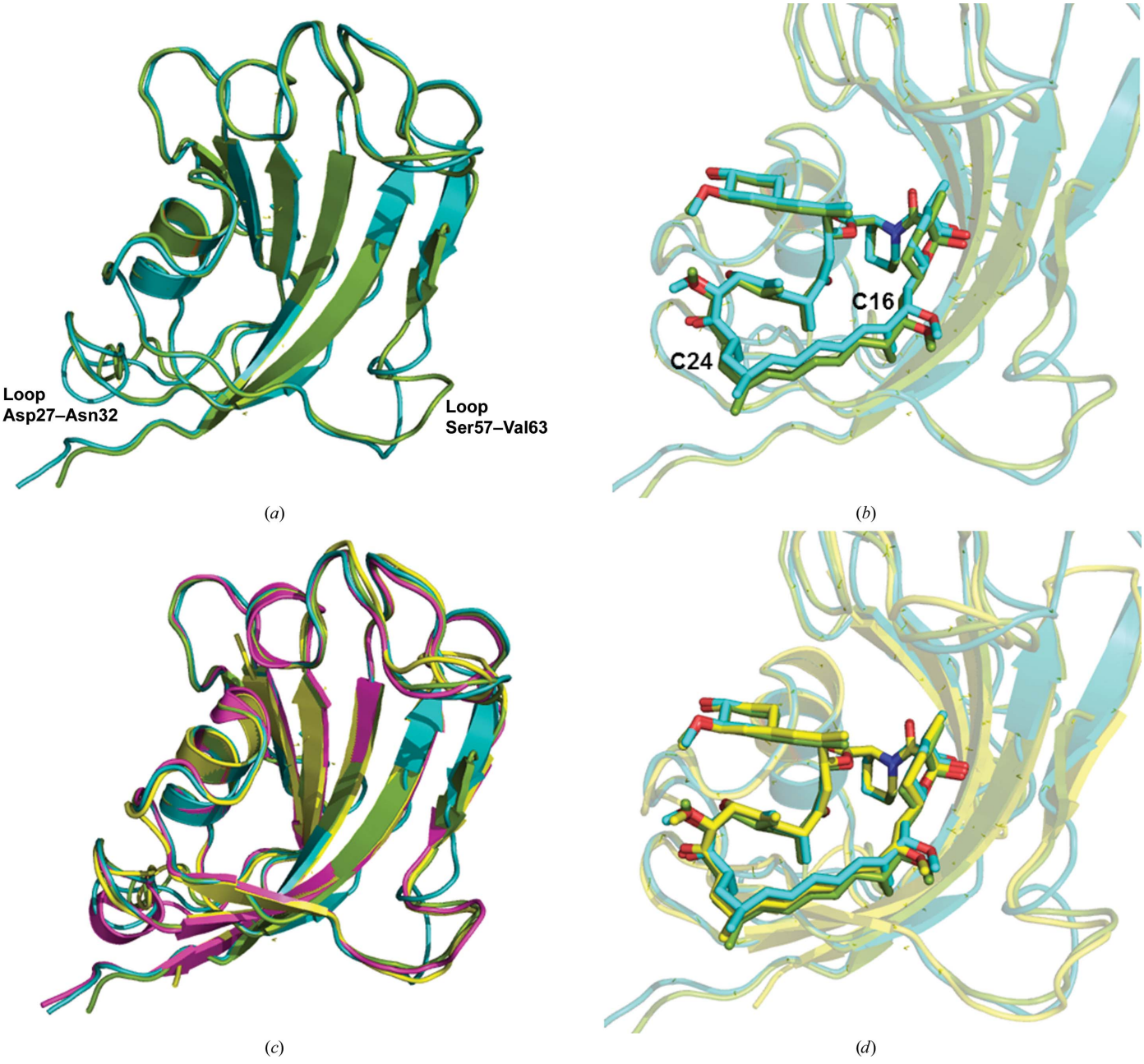

Figure 3
Structural comparison of *Pf*FKBD and hFKBP12. (*a*) Superposition of the crystal structures of the *Pf*FKBD–rapamycin complexes (PDB entry 4qt2, green; PDB entry 4qt3, cyan) showing only the protein as a cartoon representation. (*b*) Enlargement of the rapamycin in the crystal structures of the *Pf*FKBD–rapamycin complexes (PDB entry 4qt2, green; PDB entry 4qt3, cyan). (*c*) Superposition of the crystal structures of the FKBD–rapamycin complexes (PDB entry 4qt2, green; PDB entry 4qt3, cyan; PDB entry 1fkb, yellow) and *Pf*FKBD–FK506 (PDB entry 2vn1, pink) showing only the protein as a cartoon representation. (*d*) Enlargement of the rapamycin in the crystal structures of the FKBD–rapamycin complexes (PDB entry 4qt2, green; PDB entry 4qt3, cyan; PDB entry 1fkb, yellow).

major differences are found between the two structures that we obtained for *Pf*FKBD35 complexed with rapamycin. Firstly, Cys106 is covalently bonded to a molecule of dithiothreitol (DTT) in PDB entry 4qt3 and is in the reduced form in PDB entry 4qt2. The covalently bound DTT did not affect the binding mode of rapamycin (Figs. 2*c*, 2*d*, 2*e* and 3*b* and Table 2). Secondly, the loop formed by residues Ser57–Val63 indicates some conformational changes between the two structures (Fig. 3*a*). This rearrangement is owing to crystal packing and exposes the side chains of the residues of this loop differently from in the other monomer. The motion of this loop from residues Ser57 to Val63 implies different packing and explains the difference in the unit-cell parameters, where the parameter that is conserved between the two structures is *b* for 4qt2 and *a* for 4qt3. This difference slightly influences the binding of rapamycin to *Pf*FKBD35; we observed small movements in the region which links C16 to C24 of rapamycin (Fig. 3*b*) without affecting the hydrogen bonds and van der Waals interactions between rapamycin and *Pf*FKBD35 (Figs. 2*c*, 2*d* and 2*e* and Table 2). This observation is correlated with the fact that this region of rapamycin is not directly implicated in the binding interaction with *Pf*FKBD35.

3.3. Comparison of *Pf*FKBD35 with hFKBP12 in complex with rapamycin

Comparison of the primary sequence of *Pf*FKBD with that of the archetypal human FKBP protein shows that it is highly conserved (44% identity; Monaghan & Bell, 2005). An alignment of hFKBP12, *Pf*FKBD and other parasite FKBDs is shown in Fig. 1(*c*), in which identical residues are highlighted by asterisks. The contacts established between rapamycin and *Pf*FKBD are listed in Table 2, allowing direct comparison with the human FKBP12 protein (PDB entry 1fkb; Van Duyne *et al.*, 1991). Rapamycin forms hydrogen bonds to hFKBP12 active-site residues Asp37, Ile56, Gln53, Glu54 and Tyr82, which orientate the inhibitor correctly and stabilize the formation of the ternary complex; several residues are involved in hydrophobic interactions, among which His87 is the most interesting since it is not conserved in the *Plasmodium* protein. Our *Pf*FKBD–rapamycin structures superimposed on *Hs*FKBP12–rapamycin (PDB entry 1fkb, chain *A*; Van Duyne *et al.*, 1991) with an r.m.s.d. of 0.35 Å; on comparing the ligands the r.m.s.d. is 0.21 Å (Figs. 3*c* and 3*d*). The ligand surface area in hFKBP12 is 2294 Å^2. Major differences are found within the β4–β6 region, in which His87 and Ile90 in human FKBP12 are replaced by Cys106 and Ser109, respectively, in *Pf*FKBD. In the human FKBP12 protein the side chains of these two residues form a complementary surface to the pyranose moiety of rapamycin and thus play an important role in ligand binding. The *Pf*FKBP35 residues, in contrast, are not directly in contact with rapamycin since the distances between the Cys106 sulfhydryl group and the Ser109 hydroxyl group are 4.2 and 4.3 Å, respectively. The short distance of rapamycin from Cys106 may permit the design of rapamycin analogues that could react (*via* the insertion of an electrophilic group such as Br or Cl, or the introduction of a Michael acceptor on carbons 43 and 40; Fig. 4) with the cysteine in order to achieve selectivity between the human and *Plasmodium* proteins without immunosuppressive effects. The r.m.s.d.s of the proteins at their C$^\alpha$ positions are 0.31 and 0.36 Å for FKBD-1 of hFKBP51 and hFKBP52, respectively (PDB entries 4dri and 4drj; März *et al.*, 2013). These comparisons demonstrate that the same hydrogen-bond network is present in all complexes, which is in agreement with the structural conservation of the fold and the strict residue conservation in the active site.

Table 2
Interactions between rapamycin and *Pf*FKBD.

Amino-acid substitutions compared with hFKBP12 (PDB entry 1fkb) are shown in bold.

(*a*) Nonpolar contacts. Nonpolar contacts are shown for distances of <4.5 Å.

Ligand region	4qt2	4qt3	1fkb
C2	Ile75, Trp78	Ile75	Ile56
C3, C4, C5	Val74	Trp78	Trp59
C4	Phe65	Val74	Val55
C5	Val74	Phe65, Val74	Tyr26, Phe46
C6	Tyr44	Tyr44	Tyr26
C12	**Cys106**	**Cys106**	**His87**
C35	Tyr101	Tyr101	**Tyr82**
C42	Ile75	Ile75	Ile56
C43	Phe55, **Cys106**	Phe55, **Cys106**, Ile110	Phe36, **His87**, **Ile90**
C44	Phe65	Phe49, Phe65	Phe46
C46	Glu73	Glu73	Glu54
C48	Phe65	Phe65	Phe46
C49	**Cys106**, Tyr101	**Cys106**, Tyr101	Tyr82, **His87**

(*b*) Hydrogen bonds.

Ligand	*Pf*FKBD	Donor–acceptor distance, 4qt2/4qt3 (Å)	hFKBP	Donor–acceptor distance, 1fkb (Å)
C1 carbonyl	Ile75 NH	2.93/2.92	Ile56 NH	3.02
C8 carbonyl	Tyr101 OH	2.61/2.66	Tyr82 OH	2.76
C10 hydroxyl	Asp56 O$^\beta$	2.69/2.58	Asp37 O$^\beta$	2.74
C28 hydroxyl	Glu73 CO	2.75/2.74	Glu54 CO	2.84
C40 hydroxyl	**Gly72 CO**	2.80/3.23	**Gln53 CO**	2.75

3.4. Comparison with *Pf*FKBD in complex with FK506

FK506 is smaller in size than rapamycin, but the interacting part of the ligand is common between the two, and the Tanimoto score is 0.934. The residues of *Pf*FKBD that interact with rapamycin are the same residues as highlighted in the structure with PDB code 2vn1 by Kotaka *et al.* (2008) to interact with FK506 with a hydrogen-bond network involving residues Asp56, Ile75, Gly72, Glu73 and Tyr101. In this structure Cys106 and Ser109 also do not directly interact with FK506 (distances of 3.9 and 5.4 Å from FK506, respectively). *Pf*FKBD in complex with rapamycin can be superimposed on *Pf*FKBD–FK506 (PDB entry 2vn1) with r.m.s.d.s of 0.23 Å for 4qt2 and 0.19 Å for 4qt3 (Fig. 3*c*). PDB entry 4qt2 demonstrates close similarity to PDB entry 2vn1 (Fig. 3*c*), although a small rearrangement is observed in the loop formed by residues Asp27–Asn32. This conformational change is owing to the crystal packing and exposes the side chains of the residues of this loop differently from those in the other monomer. This

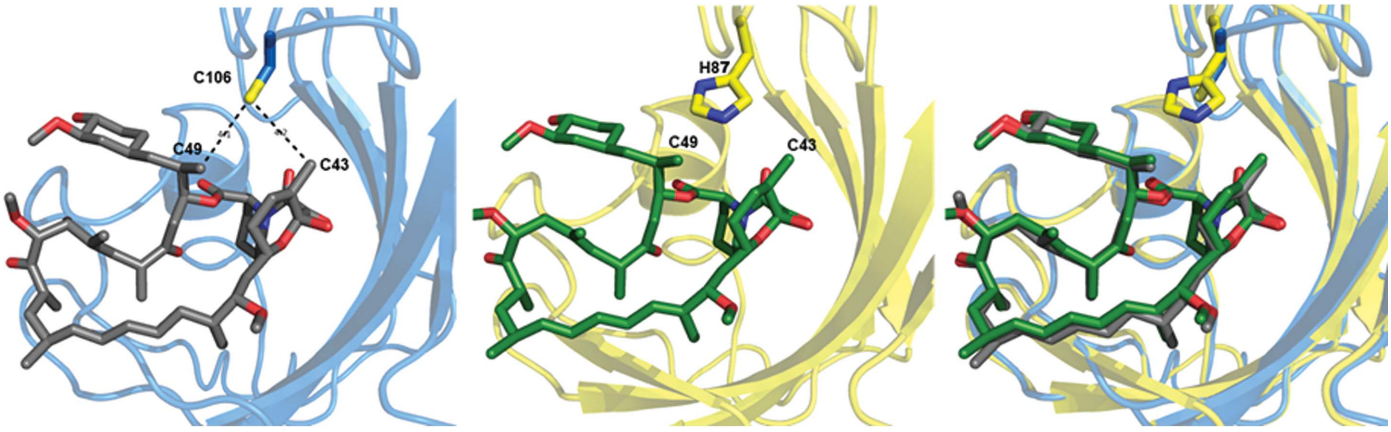

Figure 4
Structural comparison of *Pf*FKBD and hFKBP12 for the design of specific inhibitors. (*a*) Cartoon representation of *Pf*FKBD and stick view of rapamycin and residue Cys106 (PDB entry 4qt2). (*b*) Cartoon representation of hFKBP12 and stick view of rapamycin and residue His87 (PDB entry 1fkb). (*c*) Superposition of (*a*) and (*b*) (PDB entries 4qt2 and 1fkb).

region is not implicated in the binding of rapamycin or FK506. On the contrary, comparison of PDB entry 4qt3 with PDB entry 2vn1 shows a superposition of the loop formed by residues Asp27–Asn32. As observed in the comparison of 4qt2 and 4qt3, the main difference between these two structures (4qt3 and 2vn1) is a rearrangement of the loop formed by residues Ser57–Val63 (Fig. 3*c*).

4. Discussion

FKBPs have been studied for many decades owing to their interaction with macrolactones, which causes immunosuppression. The immunosuppressive drugs FK506 and rapamycin have been in use since 2005 and 2008, respectively, in immunosuppressive regimens after organ transplantation. In particular, rapamycin (which acts independently of calcineurin) is the specific drug used after kidney transplantation. FK506 and rapamycin are known to have antimalarial activity (Bell *et al.*, 1994, 2006; Monaghan & Bell, 2005; Kumar *et al.*, 2005), but the mechanism of their action in *Plasmodium* is still obscure.

Here, we present the three-dimensional structure of the *Pf*FKBP35 FKBD in complex with rapamycin at high resolution, and we are now able to compare it with the interactions between this drug and previously reported FKBDs and the interaction between *Pf*FKBD and FK506. The *Pf*FKBD–FK506 complex (Kotaka *et al.*, 2008) shows the same hydrogen-bond interactions as rapamycin, which also interacts with Gly72. Rapamycin interactions with *Pf*FKBD are mostly observed with residues conserved in hFKBP12: a total of five hydrogen bonds and several van der Waals interactions can be discriminated within the active site. Important structural differences between the *P. falciparum* and human proteins are found; for example, *Pf*FKBD Cys106 and Ser109 are replaced by His87 and Ile90 in hFKBP12. In particularly, His87 interacts with FK506 and rapamycin, orienting and stabilizing the complex. For these reasons, Cys106 can be selected as an ideal inhibitor target amino acid in the active site, as a covalent inhibitor should be specific to the *Plasmodium* form. The argument for the development of a thiol-reactive rapamycin analogue is further supported by the finding that the reduced form that contains a covalently linked DTT molecule (PDB entry4qt3) is still able to bind rapamycin, with close proximity of the DTT to its pyranose ring (see Figs. 2*d* and 4*a*). The addition of thiol-reactive groups to this region of rapamycin may yield a covalent inhibitor that shows greater specificity for the *Plasmodium* form of FKBP.

In conclusion, the results presented here highlight the necessary components of the rapamycin molecule for binding to the *Pf*FKBP35 active site and furthermore the structural differences from human proteins that might lead to the design of specific and non-immunosuppressive *Plasmodium* inhibitors.

Acknowledgements

This work was supported by the Irish Research Council (UCD Bioinformatics and System Biology PhD program), the University of Montpellier, CNRS, INSERM and the French Infrastructure for Integrated Structural Biology (FRISBI) ANR-10-INSB-05-01. We thank Dr Labesse and Dr Trapani for helpful discussion of the results.

References

Ahearn, I. M., Tsai, F. D., Court, H., Zhou, M., Jennings, B. C., Ahmed, M., Fehrenbacher, N., Linder, M. E. & Philips, M. R. (2011). *Mol. Cell*, **41**, 173–185.
Bell, A., Monaghan, P. & Page, A. P. (2006). *Int. J. Parasitol.* **36**, 261–276.
Bell, A., Wernli, B. & Franklin, R. M. (1994). *Biochem. Pharmacol.* **48**, 495–503.
Blackburn, E. A. & Walkinshaw, M. D. (2011). *Curr. Opin. Pharmacol.* **11**, 365–371.
Braun, P. D., Barglow, K. T., Lin, Y.-M., Akompong, T., Briesewitz, R., Ray, G. T., Haldar, K. & Wandless, T. J. (2003). *J. Am. Chem. Soc.* **125**, 7575–7580.
Cameron, A. M., Steiner, J. P., Sabatini, D. M., Kaplin, A. I., Walensky, L. D. & Snyder, S. H. (1995). *Proc. Natl Acad. Sci. USA*, **92**, 1784–1788.

Debreczeni, J. É. & Emsley, P. (2012). *Acta Cryst.* D**68**, 425–430.
Edlich, F., Weiwad, M., Wildemann, D., Jarczowski, F., Kilka, S., Moutty, M. C., Jahreis, G., Lücke, C., Schmidt, W., Striggow, F. & Fischer, G. (2006). *J. Biol. Chem.* **281**, 14961–14970.
Evans, P. R. (2011). *Acta Cryst.* D**67**, 282–292.
Galat, A. (2003). *Curr. Top. Med. Chem.* **3**, 1315–1347.
Harikishore, A., Leow, M. L., Niang, M., Rajan, S., Pasunooti, K. K., Preiser, P. R., Liu, X. & Yoon, H. S. (2013). *ACS Med. Chem. Lett.* **4**, 1097–1101.
Harikishore, A., Niang, M., Rajan, S., Preiser, P. R. & Yoon, H. S. (2013). *Sci. Rep.* **3**, 2501.
Jayaraman, T., Brillantes, A. M., Timerman, A. P., Fleischer, S., Erdjument-Bromage, H., Tempst, P. & Marks, A. R. (1992). *J. Biol. Chem.* **267**, 9474–9477.
Jinwal, U. K., Koren, J. III, Borysov, S. I., Schmid, A. B., Abisambra, J. F., Blair, L. J., Johnson, A. G., Jones, J. R., Shults, C. L., O'Leary, J. C. III, Jin, Y., Buchner, J., Cox, M. B. & Dickey, C. A. (2010). *J. Neurosci.* **30**, 591–599.
Kabsch, W. (2010). *Acta Cryst.* D**66**, 125–132.
Kang, C. B., Ye, H., Yoon, H. R. & Yoon, H. S. (2008). *Proteins*, **70**, 300–302.
Kantardjieff, K. A. & Rupp, B. (2003). *Protein Sci.* **12**, 1865–1871.
Kofron, J. L., Kuzmic, P., Kishore, V., Colón-Bonilla, E. & Rich, D. H. (1991). *Biochemistry*, **30**, 6127–6134.
Kotaka, M., Ye, H., Alag, R., Hu, G., Bozdech, Z., Preiser, P. R., Yoon, H. S. & Lescar, J. (2008). *Biochemistry*, **47**, 5951–5961.
Kumar, R., Adams, B., Musiyenko, A., Shulyayeva, O. & Barik, S. (2005). *Mol. Biochem. Parasitol.* **141**, 163–173.
Kuzuhara, T. & Horikoshi, M. (2004). *Nature Struct. Mol. Biol.* **11**, 275–283.
Larkin, M. A., Blackshields, G., Brown, N. P., Chenna, R., McGettigan, P. A., McWilliam, H., Valentin, F., Wallace, I. M., Wilm, A., Lopez, R., Thompson, J. D., Gibson, T. J. & Higgins, D. G. (2007). *Bioinformatics*, **23**, 2947–2948.
März, A. M., Fabian, A. K., Kozany, C., Bracher, A. & Hausch, F. (2013). *Mol. Cell. Biol.* **33**, 1357–1367.
Monaghan, P. & Bell, A. (2005). *Mol. Biochem. Parasitol.* **139**, 185–195.
Monaghan, P., Fardis, M., Revill, W. P. & Bell, A. (2005). *J. Infect. Dis.* **191**, 1342–1349.
Murshudov, G. N., Skubák, P., Lebedev, A. A., Pannu, N. S., Steiner, R. A., Nicholls, R. A., Winn, M. D., Long, F. & Vagin, A. A. (2011). *Acta Cryst.* D**67**, 355–367.
Riggs, D. L., Roberts, P. J., Chirillo, S. C., Cheung-Flynn, J., Prapapanich, V., Ratajczak, T., Gaber, R., Picard, D. & Smith, D. F. (2003). *EMBO J.* **22**, 1158–1167.
Shirane, M. & Nakayama, K. I. (2003). *Nature Cell Biol.* **5**, 28–37.
Studier, F. W. (2005). *Protein Expr. Purif.* **41**, 207–234.
Vagin, A. & Teplyakov, A. (2010). *Acta Cryst.* D**66**, 22–25.
Van Duyne, G. D., Standaert, R. F., Schreiber, S. L. & Clardy, J. (1991). *J. Am. Chem. Soc.* **113**, 7433–7434.
White, N. J. (2004). *J. Clin. Invest.* **113**, 1084–1092.
White, N. J., Pukrittayakamee, S., Hien, T. T., Faiz, M. A., Mokuolu, O. A. & Dondorp, A. M. (2014). *Lancet*, **383**, 723–735.
Winn, M. D. *et al.* (2011). *Acta Cryst.* D**67**, 235–242.
World Health Organization (2015). *World Malaria Report 2014.* Geneva: World Health Organization.http://www.who.int/malaria/publications/world_malaria_report_2014/en/.
Yang, W.-M., Inouye, C. J. & Seto, E. (1995). *J. Biol. Chem.* **270**, 15187–15193.
Yoon, H. R., Kang, C. B., Chia, J., Tang, K. & Yoon, H. S. (2007). *Protein Expr. Purif.* **53**, 179–185.